Analytical Solutions to the Collection Growth Equation: Comparison with Approximate Methods and Application to Cloud Microphysics Parameterization Schemes

JOHANNES VERLINDE,* PIOTR J. FLATAU AND WILLIAM R. COTTON

Colorado State University, Department of Atmospheric Science, Fort Collins, Colorado

(Manuscript received 24 January 1990, in final form 11 May 1990)

ABSTRACT

A closed form solution for the collection growth equation as used in bulk microphysical parameterizations is derived. Although the general form is mathematically complex, it can serve as a benchmark for testing a variety of approximations. Two special cases that can immediately be implemented in existing cloud models are also presented. This solution is used to evaluate two commonly used approximations. The effect of the selection of different basis functions is also investigated.

1. Introduction

The numerical treatment of the collection growth of precipitation particles has long been a problem in two- and three-dimensional cloud modeling. This paper examines exact and approximate solutions to the collection equation as applied to the prediction of mixing ratios of hydrometeor species in cloud models (Wisner et al. 1972; Cotton et al. 1982). The form of the collection equation that is used is the integrated form of the stochastic collection equation as applied to two different species interacting. This equation plays an important role in the bulk parameterization schemes of cloud microphysics in two- and three-dimensional cloud models, and is employed in several models currently in use (Orville and Kopp 1977; Passarelli and Srivastava 1979; Hsie et al. 1980; Cotton et al. 1982; Lin et al. 1983; Rutledge and Hobbs 1983). The solution is derived for the general form where water content may be distributed according to any of the family of gamma-type distributions. Fast solutions for self-collection as well as hail/rain interaction are obtained. Approximation schemes that are currently in use are compared to the exact solution of this integral.

The paper is organized as follows: Bulk parameterization schemes and their use in cloud and mesoscale models are discussed first. Subsequently, the collection equation defining the change in mixing ratio due to conversion between two water categories is discussed. The accretional (continuous) growth approximation and the approximation suggested by Wisner et al. (1972) are discussed there. The general solution is then derived. This is the main theoretical result of this paper. The special cases of hail collecting rain and selfcollection are also discussed. Comparisons between the approximate and the new analytical solution are given for several typical types of interactions. Finally, some discussion on the application of these results are given.

2. Bulk parameterization schemes

The primary aim of bulk parameterization schemes is to capture in a few simple formulas the essential physics embodied in more general theoretical models. It is assumed that the water content in a cloud can be categorized in different species, which, for this problem, interact through collision and coalescence. A typical division of species would be to discriminate between cloud water, rain water, pristine ice, snow/aggregates and graupel/hail. It is further assumed that for each of these categories the water content is distributed according to a specified continuous size distribution, typically one of the gamma-type family, lognormal, or even monodispersed.

The bulk microphysics approach is to assume that only the moments of size distributions such as total water content (the third moment) or the total concentration (the zeroth moment) are important for cloud evolution. Exact knowledge of the spectrum evolution is considered to be of lesser importance. Typically, only one moment of the distribution is carried as a prognostic variable in the model, although some of the more sophisticated models use two moments as prognostic variables. For a three-parameter distribution this then implies that either one or two distribution parameters have to be fixed. Equations describing the physics of the process are integrated over the assumed distribu-

* On special leave from the South African Weather Bureau.

Corresponding author address: Johannes Verlinde, Department of Atmospheric Science, Colorado State University, Fort Collins, CO 80523.

tions, and prognostic equations for the required moments are derived.

3. The collection equation and its simple approximations

The change in mixing ratio of species Y due to collisions with species X is given by the collection equation using the hydrodynamical collection kernel as

$$CL_{xy} = \frac{1}{\rho_0}\frac{\pi}{4}\int_0^\infty\int_0^\infty m(D_x)(D_x + D_y)^2 \times |v_x(D_x) - v_y(D_y)|n_x(D_x)n_y(D_y)E(x, y)dD_xdD_y. \quad (3.1)$$

In this equation CL_{xy} refers to the time rate of change of mixing ratio due to collection; $E(x, y)$ is the efficiency for which species X is collected by species Y; $m(D)$ to the mass and $v(D)$ to the terminal fall velocity. This equation is an integrated form of the stochastic collection equation for two interacting species. It has been used in cloud models as a source term in the continuity equations describing the time-varying microphysical fields. It will appear in a model formulation in the following form:

$$\frac{d\rho_0 r_x}{dt} = \cdots - \rho_0 CL_{xy} \quad (3.2)$$

and

$$\frac{d\rho_0 r_y}{dt} = \cdots + \rho_0 CL_{xy} \quad (3.3)$$

where r is the mixing ratio and ρ_0 is a reference state density.

In line with the bulk parameterization approach, we assume that each species is distributed according to a gamma-type distribution of the following form:

$$n(D) = \frac{N_t}{\Gamma(\nu)}\left(\frac{D}{D_n}\right)^{\nu-1}\frac{1}{D_n}\exp\left(-\frac{D}{D_n}\right) \quad (3.4)$$

where $n(D)$ is the number of particles with diameter D, N_t is the total number of particles, ν is the shape parameter ($\nu = 1$ for the exponential distribution) and D_n is some characteristic diameter of the distribution. This distribution is often used in atmospheric science applications. It encompasses as special cases most of the commonly used size distributions (Marshall–Palmer; Khrgian–Mazin). The D/D_n grouping is used to convert moments of the (3.4) distribution to nondimensional form. The characteristic diameter of the distribution is related to the mean diameter through

$$D_{\text{mean}} = \frac{\Gamma(\nu + 1)}{\Gamma(\nu)}D_n. \quad (3.5)$$

We will assume, according to empirical evidence (Heymsfield 1972; Locatelli and Hobbs 1974; Pruppacher and Klett 1978), that the mass and terminal velocity of each class can be expressed as a power law:

$$a = c_a D^{p_a}. \quad (3.6)$$

Here c_a and p_a are the coefficients, and a is the property we wish to define. For simplicity we assume that the collection efficiency $E(x, y) = E$ is independent of diameter; though it may depend on other factors such as ice crystal habit or temperature.

The absolute value of the difference in terminal velocities in Eq. (3.1) makes the integration cumbersome. This has lead to several approximations, including what we call the Wisner approximation.

a. The accretional growth equation

When small cloud particles (species X) are collected by bigger faster falling particles (species Y), then $v(D_y) \gg v(D_x)$ and $D_y \gg D_x$. It then follows from Eqs. (3.1) and (3.6) that the change in mass of the collector class is given by (Flatau et al. 1989):

$$CL_{xy} \approx \frac{\pi}{4} r_x N_{ty} E D_{ny}^2 v_y(D_{ny}) \times \Gamma(\nu_y + p_{vy} + 2)\Big/\Gamma(\nu_y) \quad (3.7)$$

where p_{vy} is the power coefficient of the terminal velocity of class Y, and r_x is the mixing ratio of class X, given by

$$r_x = \frac{1}{\rho_0} N_{tx} m(D_{nx})\Gamma(\nu_x + p_{mx})\Big/\Gamma(\nu_x). \quad (3.8)$$

The approximation (3.7) is essentially the same as that derived by Kessler (1969) and Manton and Cotton (1977), except that Eq. (3.7) is valid for the general family of gamma-distribution functions of which the Marshall–Palmer distribution is a special case.

b. The Wisner approximation

Wisner et al. (1972) introduced an approximation to the collection equation that became widely used in bulk microphysics models (Orville and Kopp 1977; Passarelli and Srivastava 1979; Hsie et al. 1980; Cotton et al. 1982; Lin et al. 1983; Rutledge and Hobbs 1983; Rutledge and Hobbs 1984; Cotton et al. 1986; Rutledge and Houze 1987; Farley and Orville 1986). They assumed that the terminal velocity difference $|v_x(D_x) - v_y(D_y)|$ in Eq. (3.1) can be replaced by the constant value $|v_x(D_{nx}) - v_y(D_{ny})| = \overline{\Delta v}_{xy}$.

We can then write Eq. (3.1) as

$$CL_{xy} \approx \frac{1}{\rho_0}\frac{\pi}{4} E\overline{\Delta v}_{xy}F \quad (3.9)$$

where

$$F = \int_0^\infty \int_0^\infty m_x(D_x)(D_x + D_y)^2 n_x(D_x) \times n_y(D_y) dD_x dD_y. \quad (3.10)$$

The integral F can be evaluated analytically. Upon integration we get

$$F = N_{tx} N_{ty} m_x(D_{nx}) C_{xy} \quad (3.11)$$

where the constant C_{xy} is given by

$$C_{xy} = \frac{1}{\Gamma(\nu_x)\Gamma(\nu_y)} \{ D_{nx}^2 \Gamma(\nu_x + p_{mx} + 2)\Gamma(\nu_y) + 2 D_{nx} D_{ny} \Gamma(\nu_x + p_{mx} + 1)\Gamma(\nu_y + 1) + D_{ny}^2 \Gamma(\nu_x + p_{mx})\Gamma(\nu_y + 2)\}. \quad (3.12)$$

This is the generalization of the solution obtained by Wisner et al. (1972) and Cotton et al. (1982) for raindrops colliding with hail or graupel particles.

4. General solution

We will now proceed to find the general analytical solution of the basic Eq. (3.1). Assuming that the terminal velocity can be represented in the form of a power law for both the categories, we notice that $|v_x(D_x) - v_y(D_y)|$ changes sign when

$$c_{vx} D_x^{p_{vx}} = c_{vy} D_y^{p_{vy}}, \quad (4.1)$$

and by simple manipulation of Eq. (4.1) we get

$$D_{xy} = f_{xy} D_x^{p_{xy}} \quad (4.2)$$

where

$$f_{xy} = \left(\frac{c_{vx}}{c_{vy}}\right)^{(1/p_{vy})}, \quad p_{xy} = \frac{p_{vx}}{p_{vy}} = d. \quad (4.3)$$

By doing partwise integration with respect to D_y such that the velocity difference has the same sign over each part, we can write

$$CL_{xy} = \frac{1}{\rho_0} \frac{\pi}{4} EJ \quad (4.4)$$

where

$$J = \int_0^\infty m_x(D_x)(J_1 - J_2) n_x(D_x) dD_x. \quad (4.5)$$

The integrals J_1 and J_2 are given by

$$J_1 = \int_0^{D_{xy}} (D_x + D_y)^2 [v_x(D_x) - v_y(D_y)] n_y(D_y) dD_y \quad (4.6)$$

$$J_2 = \int_{D_{xy}}^\infty (D_x + D_y)^2 [v_x(D_x) - v_y(D_y)] n_y(D_y) dD_y. \quad (4.7)$$

Integrating Eqs. (4.6) and (4.7) we get for $J_1 - J_2$

$$J_1 - J_2 = N_{ty}/\Gamma(\nu_y)\{ v_x(D_x)[D_x^2 G(0, D_{xy}) + 2 D_x D_{ny} G(1, D_{xy}) + D_{ny}^2 G(2, D_{xy})] - v_y(D_{ny})[D_x^2 G(p_{vy}, D_{xy}) + 2 D_x D_{ny} G \times (p_{vy} + 1, D_{xy}) + D_{ny}^2 G(p_{vy} + 2, D_{xy})]\} \quad (4.8)$$

where

$$G(p, q) = \gamma(p + 1, q) - \Gamma(p + 1, q). \quad (4.9)$$

Here $\gamma(a, b)$ and $\Gamma(a, b)$ are the incomplete gamma functions (Abramowitz and Stegun 1970).

From Eqs. (4.5) and (4.8) we see that the remaining integral over D_x involves expressions of the form

$$I = \int_0^\infty \tau^{\alpha - 1} e^{-b\tau} [\gamma(\nu, c\tau^d) - \Gamma(\nu, c\tau^d)] d\tau. \quad (4.10)$$

A general closed-form solution to Eq. (4.10) is derived in appendix B. Using this solution in Eq. (4.5) one gets

$$J = \frac{c_{mx} N_{tx} N_{ty}}{\Gamma(\nu_x)\Gamma(\nu_y)} D_{nx}^{-\nu_x} \Big\{ c_{vx} I\Big(p_{mx} + p_{vx} + \nu_x + 2, \nu_y, D_{nx}^{-1}, \frac{f_{xy}}{D_{ny}}, d\Big) + c_{vx} D_{ny} I\Big(p_{mx} + p_{vx} + \nu_x + 1, \nu_y + 1, D_{nx}^{-1}, \frac{f_{xy}}{D_{ny}}, d\Big) + c_{vx} D_{ny}^2 I\Big(p_{mx} + p_{vx} + \nu_x, \nu_y + 2, D_{nx}^{-1}, \frac{f_{xy}}{D_{ny}}, d\Big) - c_{vy} D_{ny}^{p_{vy}} I\Big(p_{mx} + \nu_x + 2, \nu_y + p_{vy}, D_{nx}^{-1}, \frac{f_{xy}}{D_{ny}}, d\Big) - c_{vy} D_{ny}^{p_{vy}+1} I\Big(p_{mx} + \nu_x + 1, \nu_y + p_{vy} + 1, D_{nx}^{-1}, \frac{f_{xy}}{D_{ny}}, d\Big) - c_{vy} D_{ny}^{p_{vy}+2} I\Big(p_{mx} + \nu_x, \nu_y + p_{vy} + 2, D_{nx}^{-1}, \frac{f_{xy}}{D_{ny}}, d\Big)\Big\} \quad (4.11)$$

where the function $I(\alpha, \nu, b, c, d)$ is defined in appendix B.

a. Special case of conversion between two classes for which the terminal velocity exponents are equal ($p_{vx} = p_{vy}$)

Consider the case of two hydrometeor classes with the same terminal velocity exponents ($p_{vx} = p_{vy} \equiv p_v$), which imply $d = 1$. This could be the case for similarly shaped particles like frozen raindrops, graupel particles, and rain drops. The solution is

$$J_{(p_{xy}=1)} = m(D_{nx}) \frac{N_{tx}N_{ty}}{\Gamma(\nu_x)\Gamma(\nu_y)} [v_x(D_{nx})\{D_{nx}H_1(0) + 2D_{nx}D_{ny}H_1(1) + D_{ny}^2H_1(2)\} - v_y(D_{ny}) \times \{D_{nx}H_2(0) + 2D_{nx}D_{ny}H_2(1) + D_{ny}^2H_2(2)\}] \quad (4.12)$$

where

$$H_1(n) = \frac{2}{\nu_y + n}\left(f_{xy}\frac{D_{nx}}{D_{ny}}\right)^{(\nu_y+n)} \times \Gamma(p_{mx} + p_v + \nu_x + \nu_y + 2) \times {}_2F_1\left(\nu_y + n, p_{mx} + p_v + \nu_x + \nu_y + 2; \nu_y + 1 + n; -f_{xy}\frac{D_{nx}}{D_{ny}}\right) - \Gamma(\nu_y + n)\Gamma(p_{mx} + p_v + \nu_x + 2 - n) \quad (4.13)$$

and

$$H_2(n) = \frac{2}{\nu_y + p_v + n}\left(f_{xy}\frac{D_{nx}}{D_{ny}}\right)^{(\nu_y+p_v+n)} \times \Gamma(p_{mx} + p_v + \nu_x + \nu_y + 2) \times {}_2F_1\left(\nu_y + p_v + n, p_{mx} + p_v + \nu_x + \nu_y + 2; \nu_y + p_v + 1 + n; -f_{xy}\frac{D_{nx}}{D_{ny}}\right) - \Gamma(\nu_y + p_v + n) \times \Gamma(p_{mx} + \nu_x + 2 - n). \quad (4.14)$$

Here, ${}_2F_1(\alpha, \beta; \eta; z)$ is the Gaussian hypergeometric function (Abramowitz and Stegun 1970; Luke 1977). A similar solution was found by Lo (1986) in a different context.

Equation (4.12) is difficult to use in practice in a large numerical model. The function ${}_2F_1$ is dependent on D_{nx}/D_{ny}, which varies as D_{nx} and D_{ny} are calculated from the bulk microphysics prognostic equations. It implies that H_1 and H_2 have to be calculated at each grid point and time step. In models where the mean diameter of the distribution is fixed, Eq. (4.12) can easily be used since H_1 and H_2 would then be independent of the prognostic variables and can be precalculated.

b. Special case of selfcollection

For the case of selfcollection Eq. (4.12) gives a double count for each interaction, and has to be divided by 2. This approximation would be valid for ice crystals colliding with ice crystals to form aggregates. It is also valid for models using prognostic equations for concentration of hydrometeors in which selfcollection among raindrops, aggregates, etc. is important. In that case $f_{xy}D_{nx}/D_{ny} = 1$, and H_1 and H_2 are independent of the model prognostic variables and depend only on the constant distribution parameter ν and the mass and terminal velocity exponents. Equation (4.12) then becomes

$$J_{(x=y)} = \frac{1}{2} N_t^2 m(D_n)v(D_n)D_n^2C_{xx}(p_m, p_v, \nu) \quad (4.15)$$

where

$$C_{xx} = \sum_{n=0}^{2}\left[\frac{2}{\nu + n}\Gamma(\eta)\,{}_2F_1(\nu + n, \eta; \nu + n + 1; -1) - \Gamma(\nu + n)\Gamma(p_m + p_v + \nu - n + 2)\right] + \sum_{n=0}^{2}\left[\frac{2}{\nu + p_v + n}\Gamma(\eta)\,{}_2F_1(\nu + p_v + n, \eta; \nu + p_v + n + 1; -1) - \Gamma(\nu + p_v + n) \times \Gamma(p_m + \nu - n + 2)\right] \quad (4.16)$$

$$\eta = p_m + p_v + 2\nu + 2.$$

This solution is simple since C_{xx} is a constant for any simulation, and thus needs only to be calculated once.

5. Comparisons between approximations

In this section we will compare the various approximations to Eq. (3.1) with the exact solution to this integral. The closed form solution is used to determine the exact solution. Where the closed form solution was expressed in terms of ${}_pF_q$, a numerical integration of Eq. (4.4) was performed. The numerical solutions were found to be accurate to several significant digits when compared to the closed form solutions. The comparisons are presented as

$$E_r = 10 \times \log\left(\frac{\text{approx}}{\text{exact}}\right). \quad (5.1)$$

Negative E_r indicate that the approximation is underestimating the collection, while positive values indicate overestimation.

Figure 1 presents mean terminal velocities for five classes of hydrometeors, A1, A2, B1, B2 and C1. A1

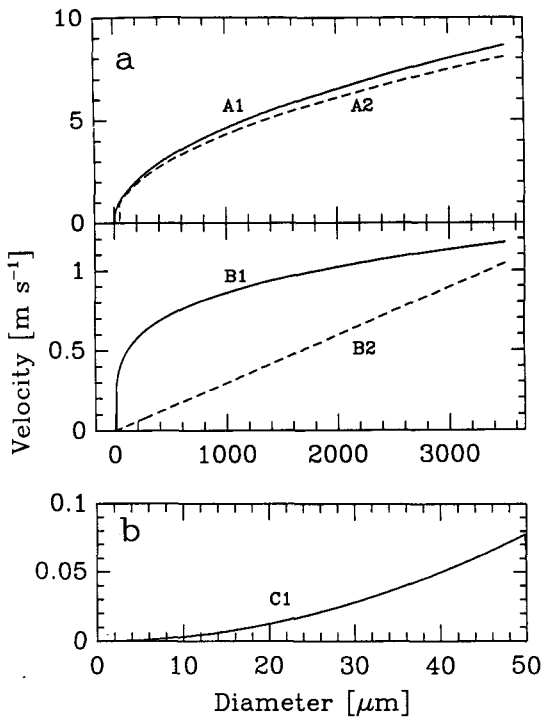

FIG. 1. Terminal fall speed dependence on diameter for (a) fast falling species A1 and A2, (b) slow falling species B1 and B2, and (c) very slow falling species C1. All species are assumed to be Marshall-Palmer type distributed.

and A2 are two fast falling classes like rain and hail. Here, B1 and B2 are two slower falling classes (typically ice classes) of which B2 has a strong diameter dependence. C1 is a slow falling class like cloud droplets.

In the calculations it is assumed that all the classes have 0.5 g kg^{-1} liquid water content distributed according to an exponential ($\nu = 1$) distribution. In addition, two gamma distributions ($\nu = 3$) were used to obtain another set of solutions, which is compared to the exponential distribution solutions. It is assumed that $E = 1$ in all calculations. However any type of polynomial dependence for the collection efficiency can easily be incorporated into the integration.

Figure 2 shows the results of the interaction between the two relatively fast falling classes A1 and A2. Panel 2a shows solutions to Eq. (3.1) for A1 collecting A2, where both A1 and A2 have exponential particle size distributions. The mass collection is on the order 10^{-6} s^{-1}, which converts to 0.6 g kg^{-1} in 10 minutes. Panel 2b shows error contours [Eq. (5.1)] between the exact and the Wisner approximation. The lighter shading indicates areas where the approximation is within 40% of the exact solution, the darker shading indicates areas where the approximation error is more than one order of magnitude. It can be seen that the Wisner approximation is valid for classes of different mean terminal velocity. It breaks down for classes with nearly the same mean terminal velocity. Notice that in this case $|v(D_{nx}) - v(D_{ny})|$ is close to 0 so that this approximation will then underestimate collection. Since the two classes may be differently distributed and may have different

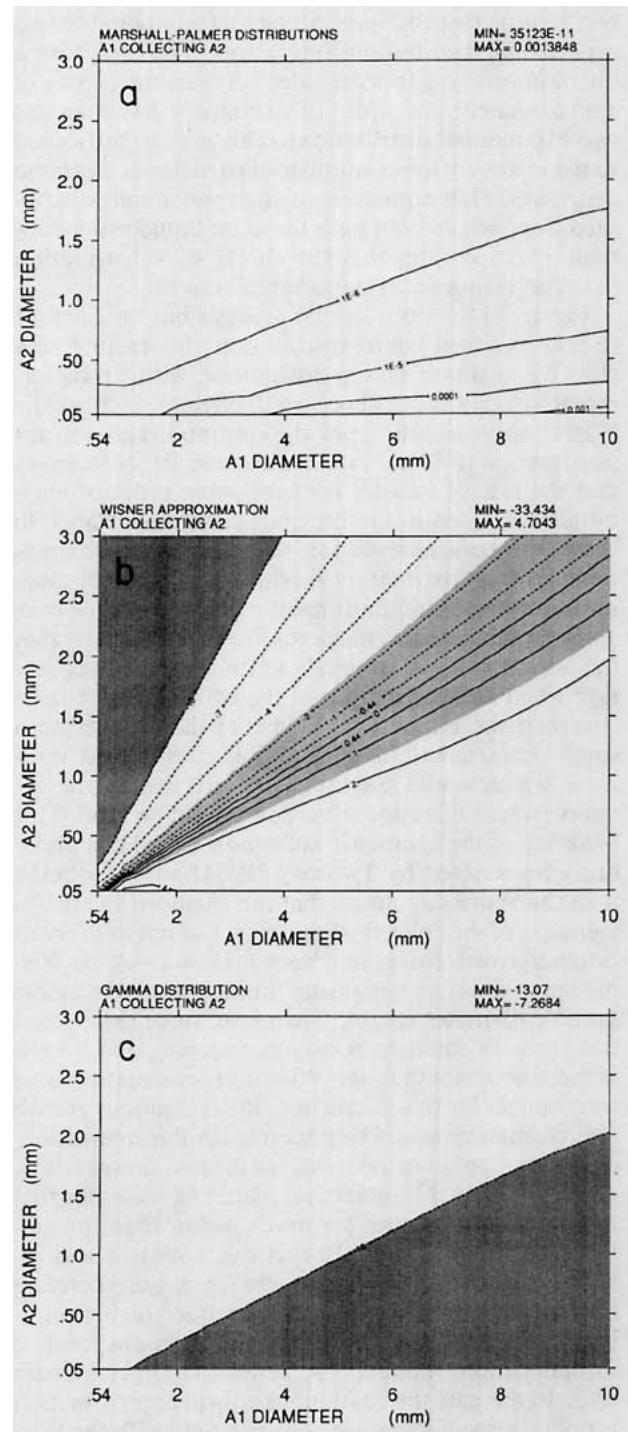

FIG. 2. Numerical integration: A1 collecting A2. Both Marshall–Palmer type distributions. (a) The mixing ratio transfer rate, (b) comparison with the Wisner approximation, (c) comparison with the two gamma distributions interacting. The light shading indicates errors within 40% of the exact solution; the dark shading errors greater than one order of magnitude.

terminal velocity dependence on diameter, the exact solution can still give a substantial transfer of mass between the two classes. The range where this approximation can be used is thus limited. Panel 2c presents two gamma distributions interacting compared to two exponential distributions interacting. The two gamma distributions give transfer rates between the classes of approximately one order of magnitude less than the two exponential distributions. This may be attributed to the relatively lower number of particles in a gamma distributed class compared to an exponentially distributed class, where both have the same liquid water content. This indicates that the choice of a distribution function is indeed an important decision.

Figure 3 presents a similar analysis but for class A1 (a relatively fast falling distribution) interacting with class B2 (a slower falling distribution with strong terminal velocity dependence on diameter). Neither the Wisner approximation nor the continuous growth approximation (3.7) are valid in this case. Panel 3a shows that the rate of transfer is of the same order of magnitude described in the previous paragraph. Panel 3b shows the error analysis for the accretion approximation. This approximation is within one order of magnitude over most of the domain and is within 40% over approximately half of the domain. It also indicates that the accretion equation tends to underestimate collection when the distribution of the collector has a large characteristic diameter and that of those collected a small characteristic diameter. This goes against intuition, which would suggest that this is exactly the situation where this approximation should be valid. This behavior of the geometric collection kernel has previously been noted by Twomey (1964) who attributed it to the statistical effects that are included in the integration of the collection equation, but not in the continuous growth equation. Panel 3c shows that the Wisner approximation has greater limitations on the usable particle diameter ranges. Therefore, since the continuous growth equation is easy to calculate, and since it is more accurate than the Wisner approximation over most ranges for this interaction, the continuous growth approximation would be preferred for this interaction.

Figure 4 presents the results of the two slower falling classes B1 and B2 interacting. Panel 4a indicates that the mass transfer rates are much higher than the previous two interactions. In this calculation it was assumed that these two classes were ice classes, therefore having lower densities, resulting in much higher number concentrations. The higher concentrations resulted in many more interactions; hence the larger transfer rates. In this case the continuous growth approximation is no longer valid, and we compare only with the Wisner approximation. Panel 4b shows that this approximation is within one order of magnitude of the exact solution over most of the domain. Once the characteristic diameters are out of that area, however, the approximation quickly deteriorates and underestimates collection by up to five orders of magnitude. Therefore, care should be used when applying this approximation in any simulation. Panel 4c shows that two gamma

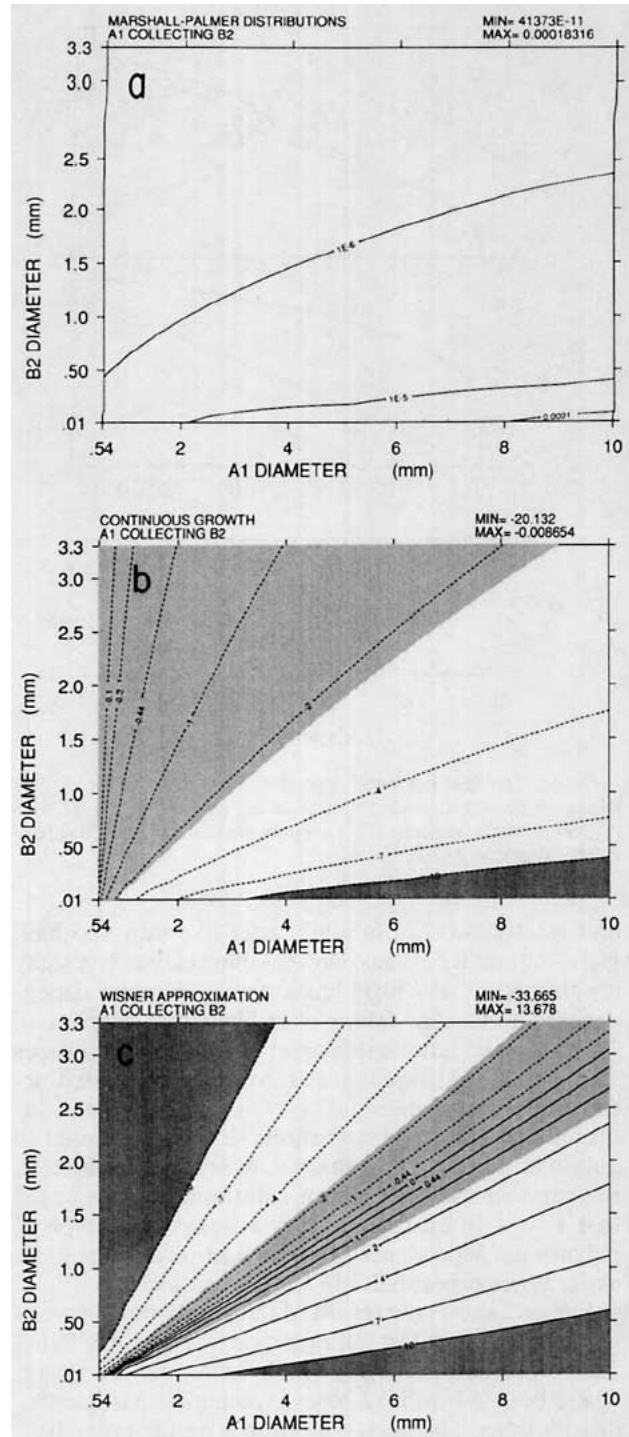

FIG. 3. Numerical integration: A1 collecting B2. Both Marshall–Palmer type distributions. (a) The mixing ratio transfer rate, (b) comparison with the continuous growth approximation, (c) comparison with the Wisner approximation. The light shading indicates errors within 40% of the exact solution; the dark shading errors greater than one order of magnitude.

distributions interacting again give lower transfer rates than the two exponential distributions interacting.

Finally, Fig. 5 will look at the process where a faster falling class B1 interacts with the slow falling class C1 (like aggregates collecting cloud droplets). The slower falling class B1 was selected over the faster falling classes A1 and A2 since it shows the limits of this approximation. Panel 5a shows that the transfer rates given by the closed form solution Eq. (4.11) are higher compared to the first two interactions considered, but lower than the two ice classes interacting. This again is a result of high number concentrations (and a collection efficiency of 1) resulting from the smaller particle sizes of the cloud droplets compared to rain drops or hail. Panel 5b shows that the continuous growth approximation gives estimates within 40% over most of the domain, with a slight overestimation for larger characteristic diameters in both classes, and large underestimations for the collected-particle distributions with very small characteristic diameters. Both species A1 and A2 gave approximations that where within 40% for all the characteristic diameters considered. Panel 5c shows that the selection of two gamma distributions will again give lower estimates for the transfer rate.

6. Discussion

This new parameterization can be implemented into existing bulk parameterization schemes with relative ease. Most two- and three-dimensional models only carry mixing ratio as a prognostic variable. In that case one parameter of a two parameter distribution, or two parameters of the three parameter distribution, have to be specified. The shape parameter ν is generally specified; if we then select the number concentration as the prognostic variable, then the characteristic diameter for each distribution has to be specified. The cumbersome bracketed expression in Eq. (4.11) [or Eq. (4.12)] can then be precalculated, since it will be a constant value (const). The general expression for the collection term is then of the form

$$CL_{xy} = \frac{1}{\rho_0}\frac{\pi}{4} E \frac{N_{tx}N_{ty}}{\Gamma(\nu_x)\Gamma(\nu_y)} c_{mx} D_{nx}^{-\nu_x} \times \text{const.} \quad (6.1)$$

This form of the equation is simple and compact.

This is also an attempt to approach the ice-phase parameterizations on a more consistent basis. The collection efficiency for the ice-phase interactions is not well defined, but it appears to be primarily dependent on habit and/or temperature. This implies that we may indeed remove it from under the integration, and multiply the calculated tendency by a value that will be determined by factors independent of the diameter.

The selfcollection parameterization can best be used in cases where the resulting outcome is best known, such as pristine ice selfcollection that produce aggregates, or rain or aggregate selfcollection that will only result in a reduction of the number concentration. To parameterize the conversion of cloud water to rain water, more assumptions have to be made since the collection efficiency among cloud droplets is known to

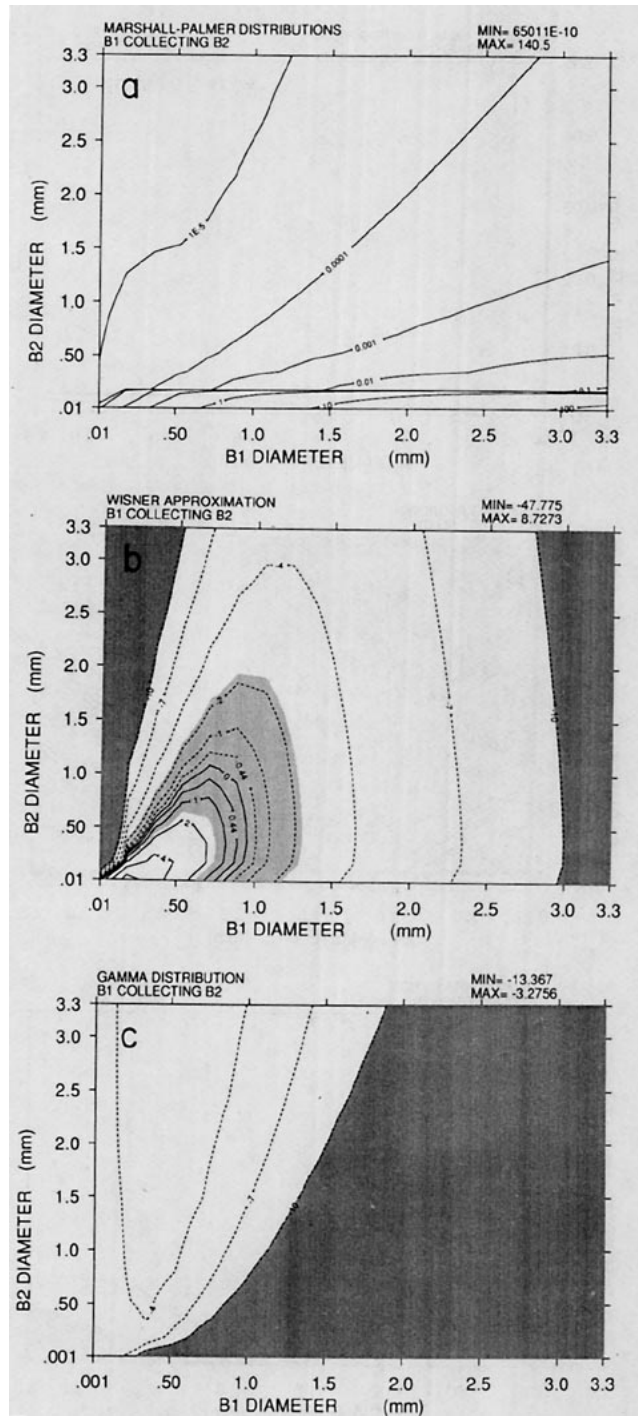

FIG. 4. Numerical integration: B1 collecting B2. Both Marshall–Palmer type distributions. (a) The mixing ratio transfer rate, (b) comparison with the Wisner approximation, (c) comparison with the two gamma distributions interacting. The light shading indicates errors within 40% of exact solution; the dark shading errors greater than one order of magnitude.

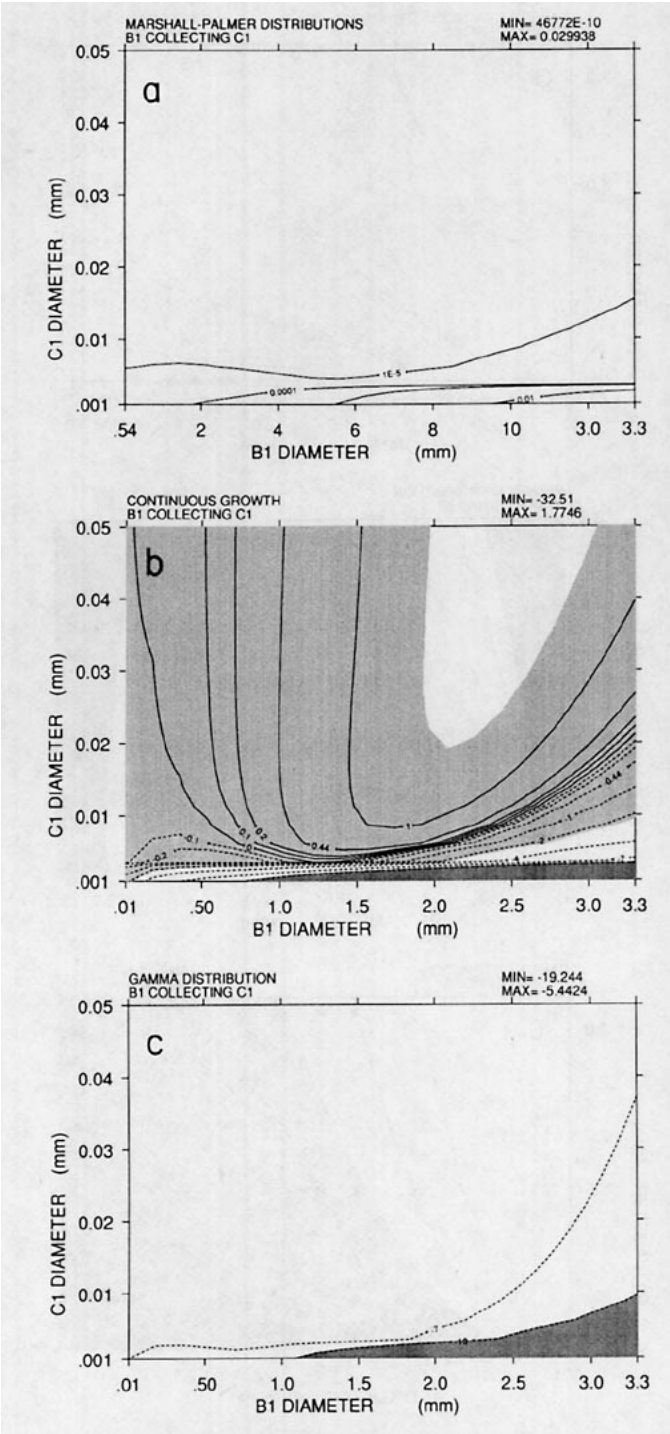

FIG. 5. Numerical integration: B1 collecting C1. Both Marshall–Palmer type distributions. (a) The mixing ratio transfer rate, (b) comparison with the continuous growth approximation, (c) comparison with the two gamma distributions interacting. The light shading indicates errors within 40% of the exact solution; the dark shading errors greater than one order of magnitude.

vary in a complicated nonlinear way, and the product of colliding cloud droplets may be classified as a cloud droplet or a rain drop, depending on the size of the colliding cloud droplets. No attempt has been made in this paper to discuss this issue, since an excellent warm rain parameterization does exist (Ziegler 1985).

7. Conclusions

An analytic closed form solution for the collection growth equation as used in bulk microphysical parameterizations has been derived. Although the general form is mathematically complex, this form can serve as a benchmark for testing many approximations for this important microphysical process. Two special cases of the general solution are also derived. These two special cases can easily be incorporated into existing cloud models.

This solution was used to evaluate two commonly used approximations, and the results indicate that careful consideration to allowable hydrometeor characteristic diameter ranges and assumed particle distributions ought to be given since these approximations can under- or over-estimate the collection process by several orders of magnitude. However, it is possible to use these previous formulated approximations, provided that certain restrictions on the allowable characteristic diameter ranges are made. It was also shown that the selection of a basis function for any given water category can greatly influence this process, therefore, careful consideration ought to be given to this decision.

Acknowledgments. The author JV was supported by the South African Weather Bureau. We thank W. J. Cody of the Argonne National Laboratory and J. R. Nickerson of the University of Toronto who both helped in our search for routines to calculate hypergeometric functions, and I. O. Marichev of Byelorussian State University for his correspondence on our solution. The research was supported in part by the Air Force Office of Scientific Research under Contract AFOSR-88-0143, in part by the Army Research Office under Contract DAAL03-86-K0175, and in part by the National Science Foundation under Grant ATM-8814913. Some of the calculations were performed on the National Center of Atmospheric Research CRAY-X-MP supercomputers. NCAR is supported by the National Science Foundation.

APPENDIX A

Notation Used in Text

In this Appendix we will describe the notations used in this paper. The notations follow the work of Marichev (1982).

The Gamma function is defined by

$$\Gamma(s) = \frac{\Gamma(s+n)}{(s)_n}$$

$$= \frac{1}{s(s+1)\cdots(s+n-1)} \int_0^\infty x^{s+n-1} e^{-x} dx. \quad \text{(A.1)}$$

The general hypergeometric function ${}_pF_q$ is defined by

$$\sum_{k=0}^{\infty} \frac{(a_1)_k(a_2)_k\cdots(a_p)_k}{(b_1)_k\cdots(b_q)_k}\frac{z^k}{k!} \equiv {}_pF_q((a);(b);z)$$
$$\equiv {}_pF_q\left(\begin{matrix}(a);\ z\\(b)\end{matrix}\right) \equiv {}_pF_q\left(\begin{matrix}a_1, a_2, \cdots, a_p;\ z\\ b_1, b_2, \cdots, b_q\end{matrix}\right). \quad (A.2)$$

Besides these definitions, and the notation used in them, we define the following symbols:

$$\Gamma\left[\begin{matrix}a_1, a_2, \cdots, a_A\\ b_1, b_2, \cdots, b_B\end{matrix}\right] \equiv \Gamma[(a);(b)]$$
$$\equiv \frac{\Gamma(a_1)\Gamma(a_2)\cdots\Gamma(a_A)}{\Gamma(b_1)\cdots\Gamma(b_B)}, \quad (A.3)$$

$$(a)+s \equiv a_1+s, a_2+s, \cdots, a_A+s, \quad (A.4)$$

$$(b)'-b_k = b_1-b_k, \cdots, b_{k-1}-b_k,$$
$$b_{k+1}-b_k, \cdots, b_B-b_k, \quad (A.5)$$

$$\sum_A(z) = \sum_{j=1}^{A} z^{a_j}\Gamma\left[\begin{matrix}(a)'-a_j, (b)+a_j\\ (c)-a_j,\ (d)+a_j\end{matrix}\right]$$
$$\times {}_{B+C}F_{A+D-1}\left(\begin{matrix}(b)+a_j, 1+a_j-(c); (-1)^{C+A}z\\ 1+a_j-(a)', (d)+a_j\end{matrix}\right), \quad (A.6)$$

$$\sum_B\left(\frac{1}{z}\right) = \sum_{k=1}^{B} z^{-b_k}\Gamma\left[\begin{matrix}(b)'-b_k, (a)+b_k\\ (d)-b_k,\ (c)+b_k\end{matrix}\right]$$
$$\times {}_{A+D}F_{B+C-1}\left(\begin{matrix}(a)+b_k, 1+b_k-(d); (-1)^{D-B}z^{-1}\\ 1+b_k-(b)', (c)+b_k\end{matrix}\right). \quad (A.7)$$

If the series converges, then $\sum_A(z)$ and $\sum_B(1/z)$ are functions of hypergeometric type. We have defined four complex vectors: the A-dimensional vector (a), the B-dimensional vector (b), the C-dimensional vector (c), and the D-dimensional vector (d).

APPENDIX B

Solutions to Integrals Used in Text

In this section we will show how the closed form solution of integrals of the form

$$I_\Gamma(\alpha, \nu, b, c, d) = \int_0^\infty t^{(\alpha-1)}e^{-bt}\Gamma(\nu, ct^d)dt \quad (B.1)$$

and

$$I_\gamma(\alpha, \nu, b, c, d) = \int_0^\infty t^{(\alpha-1)}e^{-bt}\gamma(\nu, ct^d)dt \quad (B.2)$$

can be derived. We follow the proof of theorem 22 in Marichev (1982) in this derivation.

By letting $\tau = bt$ and $B = cb^{-d}$, we can write these integrals in the following form:

$$I(\alpha, \nu, b, c, d)$$
$$= \frac{1}{b^\alpha}\int_0^\infty \tau^\alpha e^{-\tau}\left\{\begin{matrix}\gamma(\nu, B\tau^d)\\ \Gamma(\nu, B\tau^d)\end{matrix}\right\}\frac{d\tau}{\tau}. \quad (B.3)$$

We will proceed to solve Eq. (B.1). Equation (B.2) can be solved in a similar way. Noting that the images of $\Gamma(a,x)$ and e^{-x} are defined in chapter 10 of Marichev (1982), we can do the following substitutions: $a = \nu$, $r/k = -d$, $x^{-d} = B$, $p/q = 1$ and $\mu = \alpha$. This allows us to write (B.1) in the form of theorem 22 in Marichev. If we now assume that d can be written as a rational number, then we can assign integer values to r and k; $r < 0$ and $k > 0$. Let $p = q = 1$, then we can write $m = |r|$, $n = -k$, and $l = |r|$. We use the images

$$K_1(x) = \Gamma(a, x) \Leftrightarrow \Gamma\left[\begin{matrix}s+a, s\\ s+1\end{matrix}\right],$$
$$\mathrm{Re}\,s > 0, -\mathrm{Re}\,a \quad (B.4)$$

from 10.8 28(1) and

$$K_2(x) = x^\mu e^{-x} \Leftrightarrow \Gamma[s+\mu], \quad \mathrm{Re}\,s > 0 \quad (B.5)$$

from 10.3 1(1) from chapter 10 in Marichev. This defines A_i, B_i, C_i, D_i and their associated vectors as $A_1 = 2$, $(a)_1 = (0, a)$, $A_2 = 1$, $(a)_2 = (\mu)$, $C_1 = 1$, $(c)_1 = (1)$, $B_1 = B_2 = C_2 = D_1 = D_2 = 0$. The constants defined by Eq. (7.45) in Marichev are then $\nu_1 = a-1$, $\nu_2 = \mu$, $\alpha_1 = \alpha_2 = \beta_1 = \beta_2 = 1$, and M and N are given by

$$M = |r|^{\mu-3/2}k^{a-1/2}(2\pi)^{1-(k+|r|)/2}$$

and

$$N = k^{-k}|r|^{|r|}.$$

Based upon these values, we can then write Eq. (7.44) in Marichev as

$$K_0^*(|r|s) = MN^s$$
$$\times\Gamma\left[\begin{matrix}\Delta(k, -ks), \Delta(k, a-ks), \Delta(|r|, \mu+|r|s)\\ \Delta(k, 1-ks)\end{matrix}\right], \quad (B.6)$$

which defines

$$A = |r|, \quad (a) = \left(\frac{\mu}{|r|}, \frac{\mu+1}{|r|}, \cdots, \frac{\mu+|r|-1}{|r|}\right)$$
$$B = 2k, \quad (b) = \left(0, \frac{1}{k}, \cdots, \frac{k-1}{k}, \frac{a}{k}, \frac{a+1}{k}, \cdots, \frac{a+k-1}{k}\right)$$
$$C = 0$$
$$D = k, \quad (d) = \left(\frac{1}{k}, \frac{2}{k}, \cdots, \frac{k}{k}\right).$$

This implies that $A + D = |r| + k$ and $B + C = 2k$. Now we can apply Slater's theorem (theorem 17 in Marichev) and Eq. (7.46) in Marichev to get the result we want; namely,

$$I_\Gamma(\alpha, \nu, b, c, d) = \Omega(\alpha, \nu, b, r, k) \times \begin{cases} \sum_A (\tau) & \text{for } \tau > 0 \quad \text{if } A + D > B \\ \sum_A (\tau) & \text{if } 0 < \tau < 1 \quad \text{if } A + D = B \\ \sum_B (1/\tau) & \text{if } \tau > 1 \quad \text{if } A + D = B \\ \sum_B (1/\tau) & \text{for } \tau > 0 \quad \text{if } A + D < B \end{cases}, \tag{B.7}$$

where $\Omega(\alpha, \nu, b, r, k) = b^{-\alpha}|r|^{\alpha-1/2}k^{\nu-1/2}(2\pi)^{1-(k+|r|)/2}$ and $\tau = c^{-k}b^{|r|}k^k|r|^{-|r|}$.

Now we will proceed to solve Eq. (B.2). We know that

$$\gamma(a, x) = \Gamma(a) - \Gamma(a, x). \tag{B.8}$$

If we substitute this into the integral (B.2) we get

$$\begin{aligned} I_\gamma(\alpha, \nu, b, c, d) &= \Gamma(\nu) \int_0^\infty t^{(\alpha-1)}e^{-bt}dt \\ &\quad - \int_0^\infty t^{(\alpha-1)}e^{-bt}\Gamma(\nu, ct^d)dt \\ &= \frac{\Gamma(\nu)\Gamma(\alpha)}{b^\alpha} - I_\Gamma(\alpha, \nu, b, c, d). \end{aligned} \tag{B.9}$$

We then can write the integral (4.10) as

$$I = \frac{\Gamma(\nu)\Gamma(\alpha)}{b^\alpha} - 2I_\Gamma(\alpha, \nu, b, c, d). \tag{B.10}$$

To test this solution, compare this to the tabulated solution for the special case $d = 1$. Then we get $r = -1$, $k = 1$, $\Omega = b^{-\alpha}$ and $\tau = b/c$ and $A = 1$, $B = 2$, $C = 0$ and $D = 1$, $A + B = 3 > C + D$ and $A + D = 2 = B + C$. Also, $a_1 = \nu$, $b_1 = 0$, $b_2 = a$ and $d_1 = 1$. Then, when using Slater's theorem for $-\mathrm{Re}\nu < s < 0$, we get the results in Prudnikov et al. (1986).

We note from Eqs. (B.7), (A.6), and (A.7) that the most general solution is expressed in terms of the general hypergeometric function ${}_pF_q$. This function is difficult to evaluate, and we are unable to locate computer code that can calculate it. However, the special cases that are expressed in terms of ${}_2F_1$ can be evaluated (Luke 1977; Cody 1984; Wolfram 1988).

REFERENCES

Abramowitz, M., and I. A. Stegun, 1970: *Handbook of Mathematical Functions with Formulas, Graphs, and Mathematical Tables.* Dover, 364 pp.

Cody, W. J., 1984: Rendiconti del Seminario Matematico. *Convegnu su-Special Functions: Theory and Computation.* Universita'e Plolitecnico Torino, 91–116.

Cotton, W. R., M. A. Stephens, T. Nehrkorn and G. J. Tripoli, 1982: The Colorado State University three-dimensional cloud/mesoscale model—1982, part II: An ice parameterization. *J. Rech. Atmos.*, **16**, 295–320.

——, G. Tripoli, R. M. Rauber and E. A. Mulvihill, 1986: Numerical simulation of the effects of varying ice crystal nucleation rates and aggregation processes on orographic snowfall. *J. Climate Appl. Meteor.*, **25**, 1658–1680.

Farley, R. D., and H. D. Orville, 1986: Numerical modelling of hailstorms and hailstone growth. Part I: Preliminary model verification and sensitivity tests. *J. Climate Appl. Meteor.*, **25**, 2014–2035.

Flatau, P. J., G. J. Tripoli, J. Verlinde and W. R. Cotton, 1989: The CSU-RAMS Cloud Microphysical Module: General Theory and Code Documentation. [Dept. of Atmos. Science Paper 451, Colorado State University, Ft. Collins, CO 80523.]

Heymsfield, A. J., 1972: Ice crystal terminal velocities. *J. Atmos. Sci.*, **29**, 1348–1356.

Hsie, E.-Y., R. D. Farley and H. D. Orville, 1980: Numerical simulation of ice-phase convective cloud seeding. *J. Appl. Meteor.*, **19**, 950–977.

Kessler, E., 1969: On the distribution and continuity of water substance in atmospheric circulations. *Meteor. Monogr.*, No. 32, Amer. Meteor. Soc., 84 pp.

Lin, Y.-L., R. D. Farley and H. D. Orville, 1983: Bulk parameterization of the snow field in a cloud model. *J. Atmos. Sci.*, **22**, 1065–1089.

Lo, K. K., 1986: The growth of snow in winter storms: A theoretical study. *Pap Meteorol. Res.*, **9**, 1–18.

Locatelli, J. D., and P. V. Hobbs, 1974: Fallspeeds and masses of solid precipitation particles. *J. Geophys. Res.*, **79**, 2185–2197.

Luke, Y. L., 1977: *Algorithms for the Computation of Mathematical Functions.* Academic Press, 284 pp.

Manton, M. J., and W. R. Cotton, 1977: Parameterization of the atmospheric surface layer. *J. Atmos. Sci.*, **34**, 331–334.

Marichev, O. I., 1982: *Handbook of Integral Transforms of Higher Transcendental Functions: Theory and Algorithmic Tables.* Ellis Horwood, 336 pp.

Orville, H. D., and F. J. Kopp, 1977: Numerical simulation of the life history of a hailstorm. *J. Atmos. Sci.*, **34**, 1596–1618.

Passarelli, R. E., and R. C. Srivastava, 1979: A new aspect of snowflake aggregation theory. *J. Atmos. Sci.*, **36**, 484–493.

Prudnikov, A. P., Y. A. Brychkov and O. I. Marichev, 1986: *Integrals and Series.* Vol. 2 Special Integrals, Gordon and Breach Science, 750 pp.

Pruppacher, H. R., and J. D. Klett, 1978: *Microphysics of Clouds and Precipitation.* D. Reidel, 714 pp.

Rutledge, S. A., and P. V. Hobbs, 1983: The mesoscale and microscale structure and organization of clouds and precipitation in midlatitude cyclones. VIII: A model for the "seeder-feeder" process in warm-frontal rainbands. *J. Atmos. Sci.*, **40**, 1185–1206.

——, and ——, 1984: The mesoscale and microscale structure and organization of clouds and precipitation in midlatitude cyclones. XII: A diagnostic modeling study of precipitation development in narrow cold-frontal rainbands. *J. Atmos. Sci.*, **41**, 2949–2972.

——, and R. A. Houze, 1987: A diagnostic modeling study of the trailing stratiform region of a midlatitude squall line. *J. Atmos. Sci.*, **44**, 2640–2656.

Twomey, S., 1964: Statistical effects in the evolution of a distribution of cloud droplets by coalescence. *J. Atmos. Sci.*, **21**, 553–557.

Wisner, C., H. D. Orville, and C. Myers, 1972: A numerical model of a hail-bearing cloud. *J. Atmos. Sci.*, **29**, 1160–1181.

Wolfram, S., 1988: *Mathematica A System for Doing Mathematics by Computer.* Addison-Wesley, 749 pp.

Ziegler, C. L., 1985: Retrieval of thermal and microphysical variables in observed convective storms. Part I: Model development and preliminary testing. *J. Atmos. Sci.*, **42**, 1487–1509.